Theoretical and Experimental Comparison Study of Weak Point Shape Effect on Open Hole Fracturing Pressure

Dr. Murtadha J. AlTammar, Dr. Khalid M. Al-Ruwaili, Dr. Gallyam Aidagulov, Hussain K. Al-Dakheel, Dr. Devon C. Gwaba and Dr. Mustapha Abbad

Abstract /

Placing weak point(s) within the well's stimulated section can reduce fracture initiation pressure (FIP), and thereby stimulate the intervals, which otherwise could not be broken down within the pressure limits of completion and pumping equipment. In this work, two essential weak point shapes applicable to the open hole environment were considered: 360° (or circular) notches, and perforation holes. The former included blunt (U) and sharp (V) notches, while the latter were represented by single and triple in-plane perforation holes. Triple holes were 120° phased, and similar to notches, penetrated the rock within a single plane perpendicular to the wellbore. With a focus on an open hole wellbore parallel to the minimal far-field stress, these weak points were compared by their ability to initiate transverse fracture and reduce fracturing pressure.

First, FIP and initiated fracture orientations were simulated using the theoretical model, based on 3D elastic stress analysis and nonlocal rock fracture criterion. Second, performance of each weak point was tested in a series of large-scale true triaxial hydraulic fracturing experiments on cement blocks, where boreholes and weak points were casted precisely to the given shape and dimensions. Conducted lab experiments confirmed the theoretically predicted superiority of notches over holes in reducing fracturing pressure.

Introduction

In certain geomechanical settings of today's increasingly complex tight reservoirs, initiating hydraulic fractures within the pressure limits of the completion and pumping equipment becomes a challenge[1]. Placing weak point(s) within the well's stimulated section can address this high breakdown pressure issue and reduce the number of failed fracturing stages. In the context of multistage open hole fracturing[2], circular notches were proposed as such weak points to control the number and location of initiated fractures[3, 4]; and to reduce fracture initiation pressure (FIP)[5].

Considering operational aspects of cutting circular notches downhole, there is a natural question about efficiency of the circular notches in reducing fracturing pressures in comparison to other weak point types, such as discrete perforation hole(s). Also, one may ask whether sharpening the notch tip results in further FIP reduction. In this article, we present answers to these questions by conducting a theoretical and experimental study of FIP reduction achieved by weak points of various shapes.

In this work, two essential weak point shapes applicable to open hole fracturing were considered, Fig. 1: 360° (or circular) notches and perforation hole(s). The former included blunt (U) and sharp (V) notches, while the latter were represented by single and triple in-plane perforation holes. For horizontal open hole wellbores aligned with minimum far-field stress, all weak points are intended to initiate hydraulic fractures transversely to the wellbore and at lower pressure, compared to open hole wellbores without a weak point.

FIP and initiated fracture orientations were first simulated for various weak point shapes using the theoretical model based on 3D elastic stress analysis around the weakened open hole wellbore and nonlocal rock fracture criterion[5, 6]. For a consistent comparison of the FIP reduction by different weak point shapes, their geometric dimensions — width, W_n, and penetration depth, D_n — were varied in identical ranges.

The findings of the theoretical modeling of the optimal weak point shapes were validated in a series of large-scale hydraulic fracturing experiments on 24" × 18" × 18" block samples inside a true triaxial load frame. Tight and competent reservoir rock was represented by block samples molded out of high-strength cement grout, so that the borehole and weak point could be cast precisely to the given shape and dimensions. Fracturing fluid was formulated so that its composition was close to that used in the field.

Numerical Modeling

We performed a theoretical study of the FIP sensitivity to the weak point shape and dimensions based on the

following assumptions. First, a stimulated open hole section was fixed parallel to the minimum horizontal far-field stress, $\sigma_{h,min}$, and subject to a strike-slip faulting regime, $0 < \sigma_{h,min} < \sigma_v < \sigma_{H,max}$, where σ_v is the overburden far-field stress and $\sigma_{H,max}$ is the maximum horizontal far-field stress. (Hereafter, compressive stresses are positive, and tensile stresses are negative). This configuration favors placement of multiple transverse hydraulic fractures and is relevant to field cases of stages that failed due to high breakdown pressure challenges. Next, the shape of circular notches was limited to blunt U-shape and sharp V-shape notches. Notches were compared with a "1-hole" weak point containing a single perforation oriented vertically. The perforation tunnel was considered "blunt", i.e., having a cylindrical shape with a spherical tip.

Each weak point shape was characterized by its dimensions with respect to the wellbore diameter, D_W: penetration depth into the rock, D_n, and width, W_n. The D_n was the distance from the wellbore wall to the very tip of a notch or perforation. The W_n was understood in the usual sense to define the opening of a notch in the wellbore wall, which is a constant distance between notch faces for the U notch. For holes, the width was defined as a perforation diameter.

Mathematical Model for FIP

For the purposes of this work, the theoretical model posed[6] for initiation of hydraulic fracture from the notched open hole wellbore was modified to include V notches and single-hole perforations. This model was based on 3D linear elastic analysis of stress, σ_{ij}, around the wellbore at internal pressure, P_W, in infinite rock volume loaded by the far-field stresses $\sigma_{H,max}$, $\sigma_{h,min}$, and σ_v. Under the common assumptions about isotropic and homogeneous rock defined by Young's modulus and Poisson's ratio, this model yields the well-known analytical Hubbert-Willis FIP formula for an open hole wellbore without a weak point[7, 8]:

$$FIP = T_0 - \sigma_{H,max} + 3\sigma_V \quad 1$$

In Eqn. 1, *FIP* is the minimal wellbore pressure, P_w^*, at which the highest tensile tangential stress $-\sigma_{t_0}$ at the surface of the wellbore reaches the tensile strength of the rock, T_0:

$$-\sigma_{t_0} = \max\{-\sigma_t\} = T_0 \quad 2$$

For the horizontal open hole wellbore in the strike-slip regimen in Fig. 1, this corresponds to the opening of a horizontal longitudinal fracture against the intermediate stress, σ_v.

Aidagulov et al. (2015)[6] justified the need to address the effect of rock microstructural heterogeneity in building FIP predictions from small stress concentrators, such as notch tips. They did this effectively, not by considering the point value of tangential stress, but by its integral average over the certain segment, D, of the length, d_{avg}:

$$\langle\sigma_t\rangle = \frac{1}{d_{avg}}\int_{N\in D}\sigma_t(N)dl\,,\ |D| = d_{avg}. \quad 3$$

The resulting stress averaging maximum tensile stress criterion, Fig. 2, where tensile stress profiles are averaged near the borehole (red) and U-notch tip (green) to evaluate FIP and fracture opening orientation, $\boldsymbol{t}_0$.

From a mathematical (computational) standpoint, the integral average in Eqn. 3 converges to the stress value at the surface point when $d_{avg} \to 0$. In other words, the FIP predictions based on the nonlocal stress averaging maximum tensile stress criterion converge to the local maximum tensile stress values based on Eqn. 2, as $d_{avg} \to 0$.

Application of this model to an open hole wellbore with weak points requires stresses to be solved numerically. In this regard, the boundary element method (BEM) model built[6] for U notches was a natural and straightforward choice to accurately calculate the stress concentrations near the tips of V notches in this study. This was accomplished by transforming the U-notch into a V-notch geometry by reducing the notch tip radius to a tiny value of $\rho = R_W/100$, while keeping the notch width the same (R_W is a wellbore radius). Also, the boundary mesh on the notch faces was refined toward the notch tip in the radial direction, Fig. 3.

Stresses for the single-hole perforation were computed using the finite element method (FEM) of the COMSOL Multiphysics® software. Due to symmetry, the solution was only required in a quarter of the domain, with the

Fig. 1 *The open hole weak point shapes considered in this article: circular U and V notches, single 1-hole and triple 3-hole perforations. The single hole and V-notch images are enlarged to show the weak point dimensions: depth (D_n) and width (W_n).*

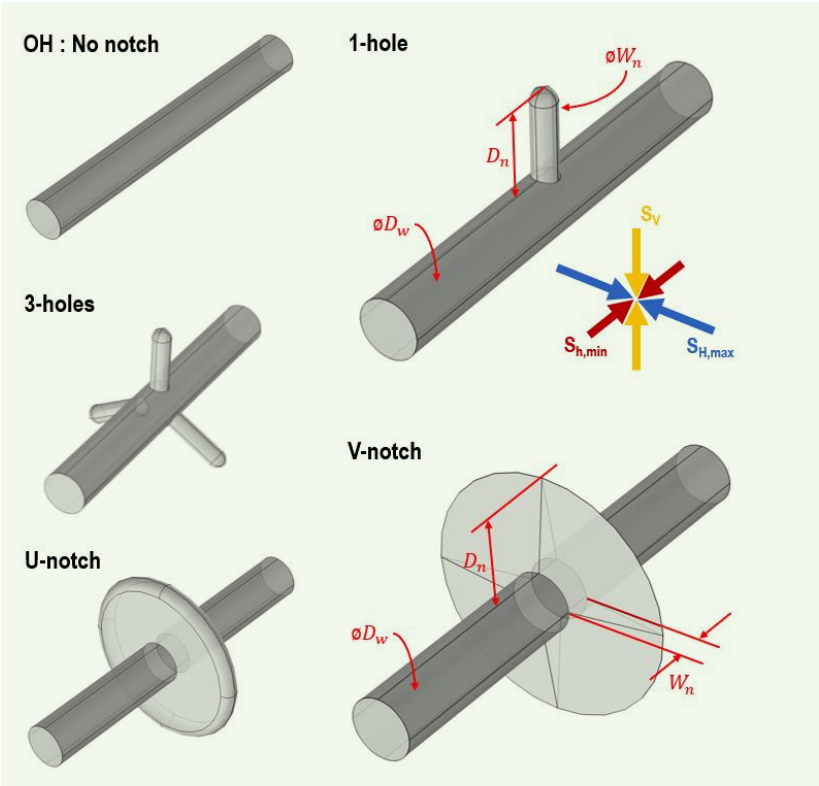

Fig. 2 *The conceptual illustration of stress averaging in the stress averaging maximum tensile stress fracture criterion applied in the 3D case to a point, M_1, at the notch tip and point M_2 at the wellbore wall.*

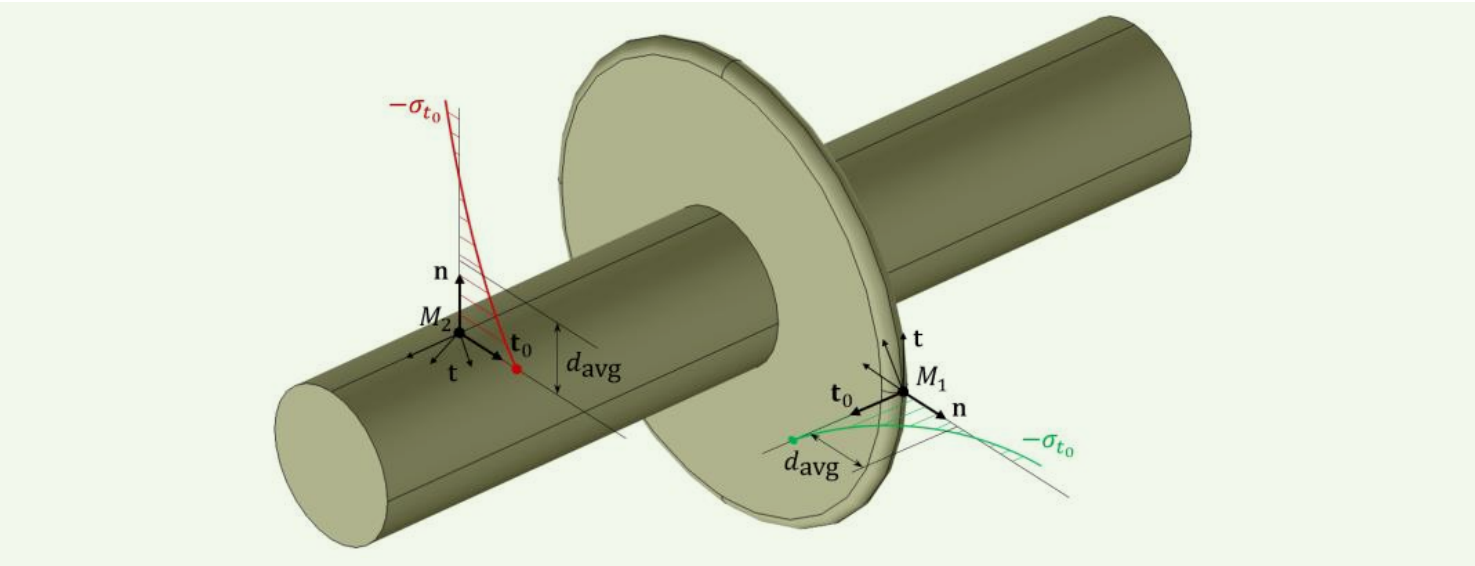

mesh refined in the vicinity of the perforation, Fig. 4.

Following Aidagulov et al. (2021)[5], we benefited from the certain FIP model features to simplify the sensitivity study:

- Linearity of the model implies that for any given surface point, M_0, and tangential vector, t_0, the stress averaging maximum tensile stress-based FIP value needed to open a fracture along t_0 is a linear combination of stresses and tensile strength:

$$\text{FIP} = \bar{D}_T T_0 + \bar{D}_H \sigma_H + \bar{D}_h \sigma_h + \bar{D}_V \sigma_V \quad (4)$$

where:

$$\bar{D}_H + \bar{D}_h + \bar{D}_V - \bar{D}_T = 1. \quad (5)$$

The stress concentration coefficients, D_α, in Eqn. 4, are expressed using the integral average of the solution components $\langle \sigma_{t_0} \rangle$ at point M_0 obtained for four specific combinations of boundary conditions. Besides being a function of point M_0, the coefficients D_α depend on:

$$\bar{D}_\alpha = \bar{D}_\alpha(\xi, \eta, \nu, \gamma) \quad (6)$$

where $\xi = D_n/_{\text{RW}}$, $\eta = W_n/R_W$, and $\gamma = d_{avg}/R_W$ are the weak point dimensions and stress averaging length normalized by the R_W. The coefficients $\bar{D}_\alpha$ in Eqn. 6 do not depend on Young's modulus not by chance, but due to isotropy assumptions of the elastic model.

It should be noted that the FIP formula in Eqn. 4 is a generalization of Eqn. 1 to the case of an arbitrary point on the wellbore surface or a weak point and nonzero d_{avg}. Indeed, Eqns. 1 and 4 are derived assuming the same physics of fracture initiation.

- A 3D stress solution around the weakened wellbore has certain symmetries, which suggest several points on the boundary of the main wellbore, circular notch, or perforation hole where it is reasonable to expect fractures to initiate.

Fig. 3 *The dissected surface of the wellbore and V notch showing BEM mesh used in FIP predictions ($\rho = R_W/100$). For notch visualization purposes, BEM mesh elements are colored here according to the distance from the wellbore.*

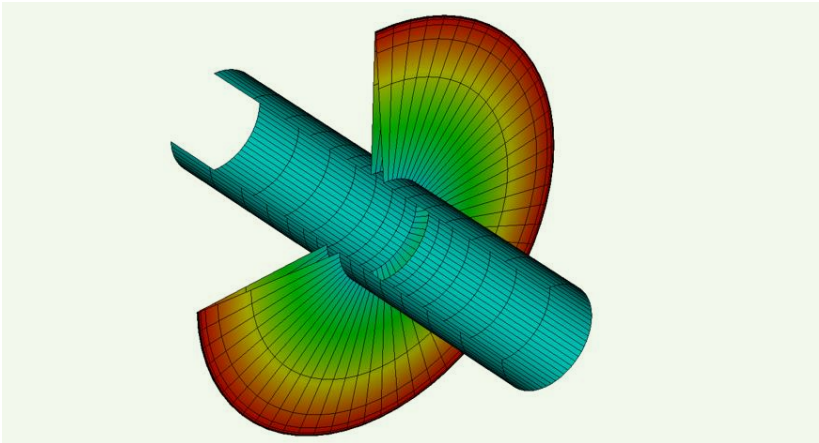

Then, the FIP value can be quickly determined as a minimum among FIPs calculated for each of these suggested points and tangential vectors. Locations of these points are defined in Fig. 5 and Fig. 6 for circular notches and a perforation hole, respectively.

Numerical Results

To discuss numerical results, we begin with the case of the open hole wellbore in Fig. 1 subjected to the stresses:

Fig. 4 *The 3D FEM simulation of the single-hole perforation. The zoomed image demonstrates a very fine mesh in the perforation vicinity to capture large stress gradients.*

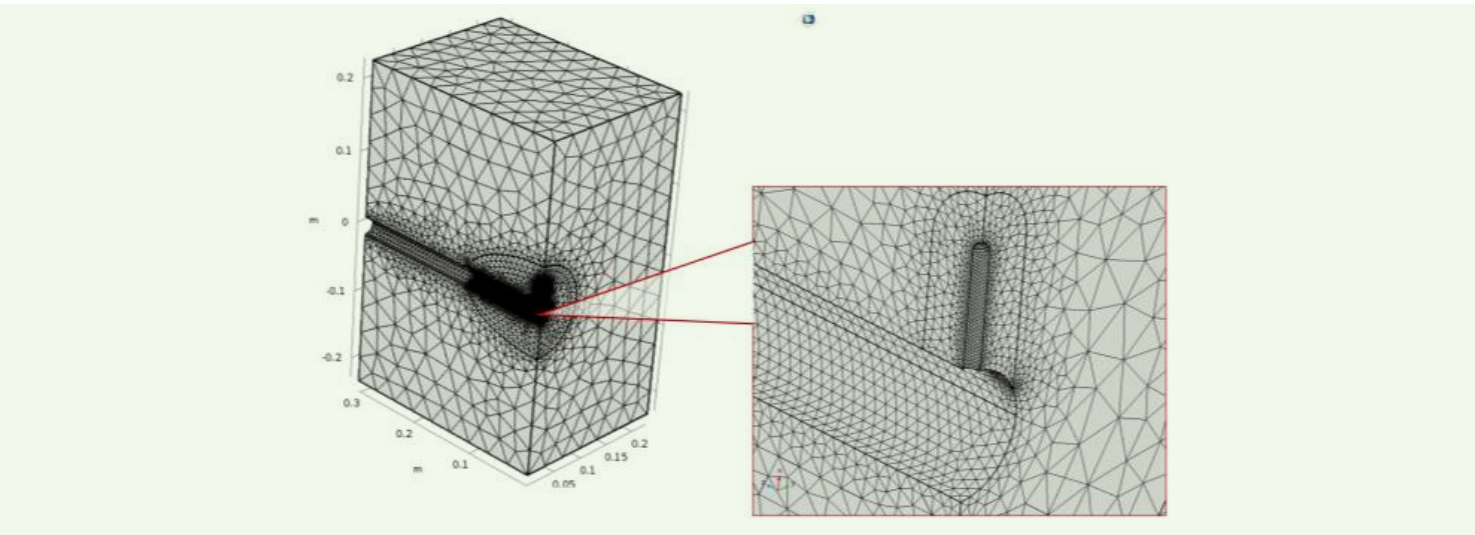

$$\sigma_{H,max} = 2{,}625 \text{ psi}$$
$$\sigma_V = 2{,}250 \text{ psi}$$
$$\sigma_{h,min} = 1{,}688 \text{ psi} \quad (7)$$

These stress values correspond to the open hole wellbore in strike-slip regimen that will be simulated in the hydraulic fracturing tests. These experiments were conducted on cement grout blocks with an average tensile strength measured at = 560 psi. A normalized width parameter of η = 0.8571 corresponds to the casted notches and perforation holes. An average reasonable Poisson's ratio of ν = 0.17 was assumed for cement grout. An averaging length parameter was selected as γ = 0.1 (or 1.6 mm), as the value that delivers the best fit to the observed FIP and fracture orientations.

The computed FIP values for various normalized D_n ξ are shown in Fig. 7.

In Fig. 7, one can see that in the absence of weak points, the FIP for an open hole is predicted at 5,016 psi, at which pressure a horizontal longitudinal fracture initiated against the intermediate vertical stress, σ_v. Introduction of the single vertical perforation decreased the predicted FIP to a range between 4,225 psi and 4,430 psi, which is a ~14% drop from the open hole value. It should be noted that the transverse fracture was initiated only for the longest perforation of three wellbore radii depths — 150% D_w.

Shorter perforations (ξ = 1 and 2) also initiated fractures but longitudinal ones occurred only at the base of the perforation. These were vertical fractures initiated against the $\sigma_{H,max}$, which were not expected to propagate far. Neglecting these fractures will open chances for transverse fractures to initiate at other locations on the perforation surface, but at pressures closer to the open hole FIP value.

On the contrary, FIP predictions for notches were completely unambiguous. For the whole range of D_n, notches initiated transverse fractures against the $\sigma_{h,min}$, with the deepest notches reducing FIP to a range between 2,258 psi and 2,494 psi or a 47% reduction from the open hole value. This indicates circular notches as a more efficient weak point than 1-hole, in terms of FIP reduction. The FIP for sharp V notches were predicted lower than for U notches, although the difference diminished as the D_n increased. Overall, the FIP for V notches was less dependent on D_n, which implied that achieving the FIP reduction of the shallowest V notch

Fig. 5 *Points 0 and 1 at the tip of the circular notch where the axial stress σ_{zz} is analyzed to check if the transverse fracture opens at these points. For notch visualization purposes, BEM mesh elements are colored here according to the distance from the wellbore.*

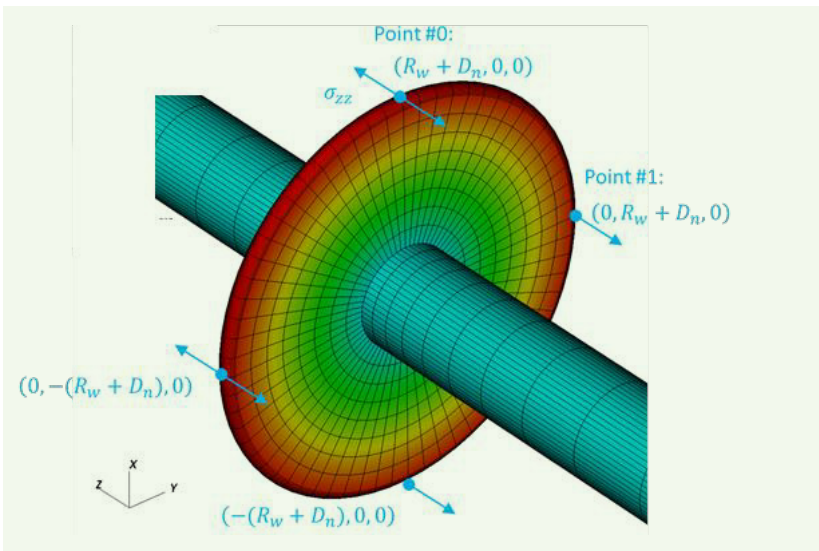

Fig. 6 *Highlighted with red color are nine points at the surface of the single-hole perforation where the corresponding tangential stress component is checked for fracture initiation.*

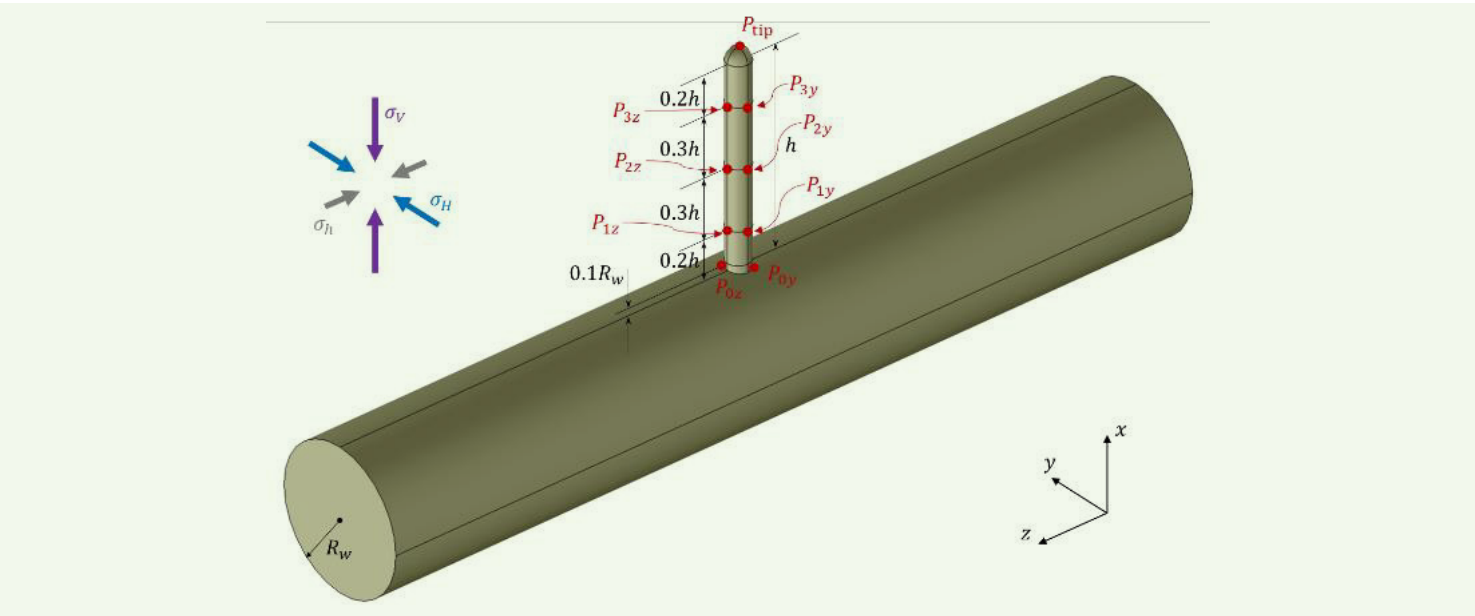

($\xi = 1$) required the deepest U notch to be $\xi = 3$. This observation suggests that it can be sufficient to ensure a sharp tip of the notch rather than making a very deep blunt-ended notch.

Experimental Study

Hydraulic fracturing experiments in this study were conducted using a large, true triaxial load frame system. Besides having the ability to apply three independent confining stresses, the load frame is equipped with pore pressure and borehole injection systems and has been used to conduct large-scale laboratory simulations of hydraulic fracturing[5] and matrix acidizing reservoir stimulation processes[9, 10].

Block Construction

The experimental samples were rectangular blocks with dimensions of 24" × 18" × 18" (0.61 m × 0.46 m × 0.46 m height, width, and depth, respectively), which is the standard size for the load frame chamber. As the focus of the present study was on the effect of the weak point shape and dimensions on the FIP, the notches and perforation holes had to be implemented in the blocks to the specified dimensions with a high degree of accuracy.

The high-pressure water jetting method[5], to cut notches in natural Indiana limestone blocks — although it was shown to be robust and mimicked field practices — could not provide the accuracy now required. That is why we decided to use artificial blocks molded from cement to benefit from precise casting of weak points. Another advantage of the cement blocks was in material homogeneity and repeatability required for consistent comparison of weak points tested in different blocks. That was achieved by strictly following the same protocol and controlling the conditions under which the blocks were manufactured.

Fig. 7 *The FIP predicted for the hydraulic fracturing test conditions in this study. The FIP values for baseline open hole (yellow), 1 hole (red), U (blue) and V notches (green) — are plotted vs. penetration depths normalized by wellbore radius. FIP values for longitudinal and transverse fractures are differentiated with triangles and circles, respectively.*

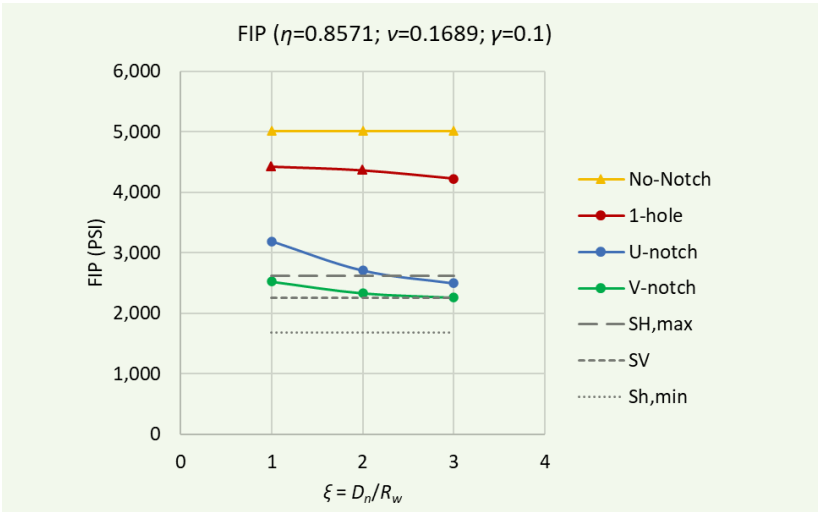

Similar to the civil engineering domain, where cement compressive strength is measured on precisely molded 2" (50 mm) cubic samples, our blocks, although being almost 1,000 times larger by volume, had to be made to meet strict requirements in terms of flatness, parallelism, and orthogonality of the faces. Indeed, blocks that do not meet such geometrical standards would develop

artifacts of nonuniform stresses and premature fractures. To avoid these artifacts in experimental data, the blocks were cast in a precisely machined steel mold with 1" (25.4 mm) wall thickness, Fig. 8.

The borehole and weak point cavities were molded inside the blocks using household candle wax. First, the complete, smooth borehole wax structure was assembled from smaller, precisely molded modules. Then the prepared borehole structure was fixed inside the large block mold, Fig. 8, followed by pouring the flowable cement mixture. After the block completed its curing time, the water inside the curing tank was gradually heated to a range of 55 °C to 60 °C, which was sufficient for the wax to soften and melt. Most of the wax melted and floated out of the borehole to the water surface. Removing the softened wax from the weak point tips and the borehole surface was completed by low-pressure jetting of water at the same temperature, Fig. 9.

We used a commercially available cement grout product supplied as a dry mixture. The required high flowability, non-shrink performance during curing, and high compressive strength of 9,000 psi were confirmed in block casting trials. The size of aggregate particles was also small compared to the cast weak points features, Fig. 9, which served as a decisive argument against micro concrete alternatives.

Cement grout is a tricky material, as opposed to well-settled natural rocks — it can develop shrinkage cracks during and after curing in response to ongoing chemical reactions and changing moisture levels. Having any preexisting cracks in the block samples would be a clear artifact and compromise our experimental results.

Considering the size of the block samples in this study, casting a solid cement part without steel rebar, or adding large aggregates (as with concrete) is a challenge not normally faced in construction or downhole cementing. Nevertheless, after a few trials, the authors established the protocol to provide the proper samples for block testing. Specifically, it was accomplished using a large 250-L paddle mixer, respecting strictly the recipe, mixing, and pouring times to avoid material bleeding and segregation. The blocks were cured and stored under water to stay moist until the exact time that they were needed for casing and testing.

Finally, Fig. 10 is a schematic of the block samples. The diameter of the borehole was 1.25" (0.032 m). In this study, we used a block with a borehole passing through the complete block from the top to bottom faces. That required installation of two casing tubings, each having an outer diameter of 1" (0.025 m), which were installed in the respective top and bottom 6" (0.15 m) sections of the borehole using high-strength epoxy. The fracturing fluid was injected from the top casing tubing. The bottom casing was closed with a flush plug. This borehole configuration was symmetric and prevented fracture artifacts, which appeared during the injection due to the stress concentrations in the bottom section of the borehole when the previous, partial, and single casing borehole configuration (not shown in this article), was applied to the cement grout samples. This left a 12"

Fig. 8 *A large block mold inside the curing tank ready for pouring the cement grout. The wax structure is installed to cast the borehole with a weak point (shown here by U-shape circular notch).*

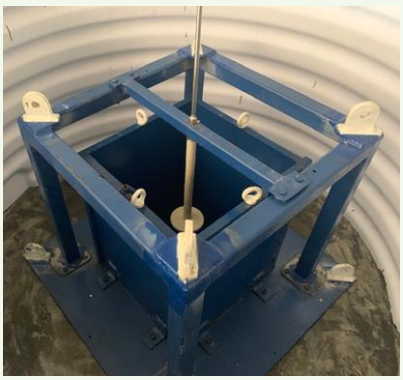

Fig. 9 *The dissected section of the trial cement grout block showing the cast borehole and V-shaped circular notch. The borehole and notch are free of wax with only a few visible traces left, which are negligible for experimentation.*

Fig. 10 *A cross section schematic of the block sample. The circular V notch is shown in the center of the open hole section. The three directions of applied confining stresses are noted with arrows.*

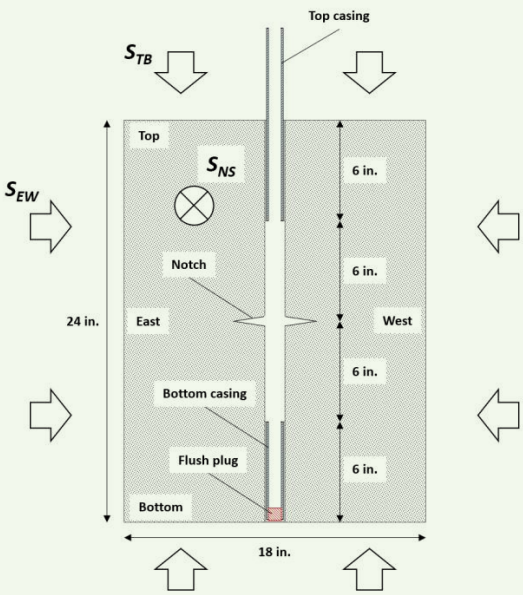

(0.31 m) long open hole section in the center of the block sample. Depending on the test, the open hole section was cast with or without a weak point in its center. The latter is demonstrated in Fig. 10 by the example of a V notch.

Test Setup

The prepared block sample was placed inside the load frame chamber and the specified values of confining stresses were applied. From then on, the confining stress system controlled the given values of confining stresses over the course of the fracturing injection to follow. Hereafter, the applied confining stresses are denoted according to their position in the setup: east-west (S_{EW}), north-south (S_{NS}), and top-bottom (S_{TB}), as previously shown in Fig. 10. The stress S_{TB} applied along the borehole was set as the minimal one, out of the three confining stresses. That represented an open hole wellbore directed along the minimum horizontal far-field stress direction.

Fracturing fluid was injected into the borehole at the fixed rate of 30 ml/min, increasing the borehole pressure, which led to initiation and growth of the hydraulic fracture. For the purposes of this study, we utilized the actual pad fluid used in the field, but with the recipe designed to have an apparent viscosity of 1,000 cP consistently between the tests.

Gas permeability measurements conducted on the cement grout cores returned zero permeability. This simulated a tight reservoir formation. Eliminating fracturing fluid leakoff in the experiment allowed us to investigate only the effect of weak point geometry on fracture initiation.

Block Testing Results

All five borehole configurations from Fig. 1 were tested in hydraulic fracturing experiments. Compared to the numerical modeling phase of the study, these included one extra 3-hole (triple) weak point configuration with the objective to see if it could deliver lower fracturing pressure than a 1-hole weak point. All perforation tunnels in the triple-hole weak point were identical and phased 120° around the wellbore. Similar to the notches, all three perforations penetrated the rock within a single plane perpendicular to the wellbore. And, just as in the 1-hole tests, one perforation out of three was directed along the vertical stress S_{EW}.

All test conditions in this work were fixed, as summarized in Table 1, except the weak point configuration. In total, we report the results of five experiments, each to test a particular weak point type and to study its effect on the initiation of hydraulic fractures (orientation and pressure). This included one baseline test with an open hole without any weak point (unnotched open hole).

Figure 11 shows the borehole injection pressures measured during fracturing fluid injection phases in each of the five experiments. Here, pressure curves are overlapped to demonstrate the excellent match of the linear borehole loading portions of the curves, to indicate consistency of the test conditions. In the analysis of pressure data, we distinguish fracture breakdown pressure (FBP) from the FIP. FBP is the maximum recorded pressure. FIP corresponds to the critical borehole pressure at which the incipient fracture occurred and

Table 1 *A summary of the test conditions.*

Block sample material		High-strength cement grout
Block sample dimensions		24″ × 18″ × 18″ (0.61 × 0.46 × 0.46 m)
Borehole diameter (wellbore)		1.25″ (32 mm)
Open hole section length		12″ (0.3 m)
Weak Point	Shape	• Baseline open hole
		• U notch
		• V notch
		• 1 hole, along SEW
		• 3 holes, one along SEW
	Width	0.55″ (14 mm), $\eta = 0.875$
	Penetration depth	1.89″ (48 mm), $\xi = 3.0$
Fracturing fluid		Fracturing pad fluid, 1,000 cP
Fluid injection rate		30 ml/min
Confining stress	S_{TB}	1,688 psi (11.6 MPa)
	S_{EW}	2,250 psi (15.5 MPa)
	S_{NS}	2,625 psi (18.1 MPa)

Fig. 11 *The hydraulic fracturing block tests. Borehole injection pressures measured during fracturing fluid injection phases in each of the five experiments as a function of time.*

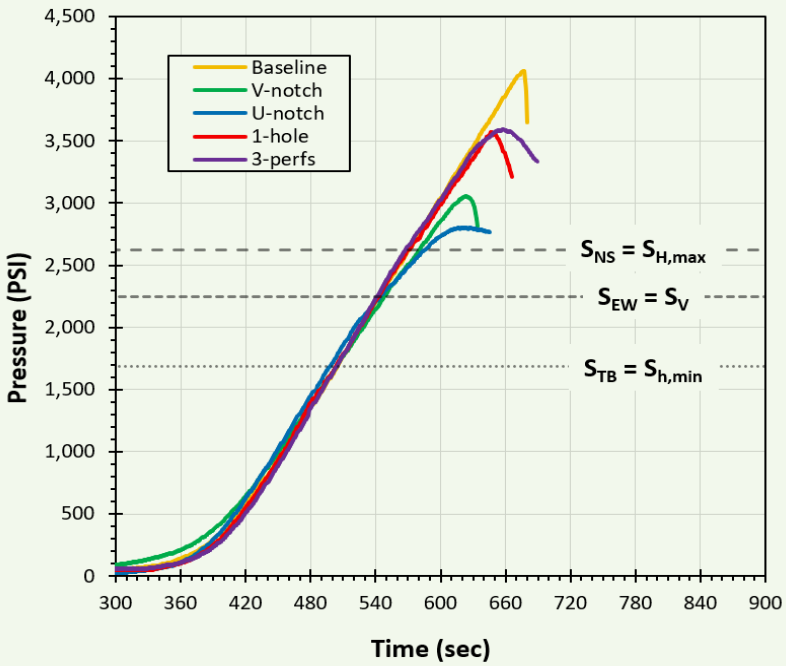

is predicted by the abovementioned theoretical model. The difference between FBP and FIP is attributed to fluid-rock interactions during the early growth of the hydraulic fracture. We estimated FIP as the pressure value at the moment when pressure started to deviate significantly from the straight line[4, 5].

To confirm the orientation of initiated fractures, portions containing weak points were extracted from the borehole vicinity by drilling 4" plugs. Figure 12 shows the longitudinal (L) fracture initiated along the borehole axis in the baseline open hole test. This fracture initiated against the intermediate stress S_{EW}, despite the fact that the borehole was oriented along the minimal stress. In the remaining four tests involving weak points, fractures were initiated from the weak point transversely (T) to the borehole against the minimal stress S_{TB}.

Figure 13 demonstrates this for the 1-hole weak point test (AUN-004 block). This is consistent with the finding previously made by the authors for circular notches in Indiana limestone[5]. Table 2 summarizes the experimental observations.

Contrary to theoretical predictions, the V-notch test (AUN-003) demonstrated approximately 10% higher FIP and FBP values than the U-notch test (AUN-001). We attribute this to natural variability observed in destructive testing, and instead consider the experimentally obtained FIP and FBP results as close to the ones predicted by the model.

The theory overestimated the FIP for baseline open hole and 1hole cases. The model predictions were obtained for d_{avg} = 1.5 mm, which is much smaller than the value

Fig. 12 *A closeup photo of the 4" central core extracted from the AUN-002 block (baseline open hole). The core came apart along the longitudinal fracture.*

of 9.5 mm[5] in modeling the FIP in hydraulic fracturing experiments in Indiana limestone. This is reasonable considering microstructural differences between the two materials. Further reduction of d_{avg} will make FIP predictions for an open hole and 1 hole closer to experimental observations and cause underestimating of results for notches. Most importantly, we believe that overall U- and V-notch experiments showed a FIP reduction of 40%,

Fig. 13 *A closeup photo of the 4" central core extracted from the AUN-004 block (1-hole). The core fell apart along the transverse fracture initiated at the perforation hole.*

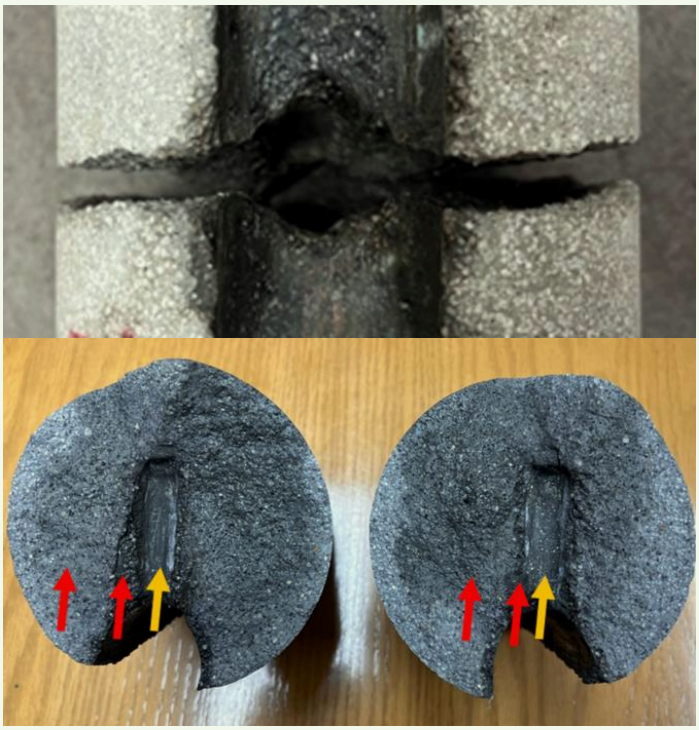

Table 2 *A summary of the experimental results.*

Block ID	Borehole/Weak Point Configuration	Fracture Orientation	FIP (psi)	FBP (psi)	FIP Reduction
AUN-002	Baseline Open Hole	L	3,950	4,060	—
AUN-001	U notch	T	2,250	2,803	43%
AUN-003	V notch	T	2,450	3,053	38%
AUN-004	1 hole	T	3,000	3,570	24%
AUN-005	3 holes	T	2,975	3,590	24%

which is consistent with the FIP reduction predicted by the theory — 47%.

Surprisingly, the 1-hole (AUN-004) and 3-hole (AUN-005) tests shown practically identical FIP and FBP, indicating that adding two more in-plane perforations did not affect fracturing pressure.

Conclusions

Several weak point shapes applicable to an open hole environment were studied — both theoretically and experimentally in the lab — for their efficiency in reducing FIP. For the experimental conditions considered in this article to mimic stimulation of a horizontal open hole wellbore in strike-slip stress regimen, the following conclusions can be drawn:

- Consistent with theory, baseline testing of an open hole without a weak point produced a nonplanar tortuous fracture that initiated longitudinally.
- In all lab tests with weak points, including both notches and perforations, initiation of the transverse fractures was observed, consistent with theory.
- Lab tests confirmed theoretically predicted superiority of notches over (vertical) perforations in reducing the FIP.
- U and V notches of 150% $D_W D_n$ were found similar experimentally and reduced FIP and FBPs by 40% and 27%, respectively, compared to the baseline open hole.
- Lab tests with single and three in-plane perforations

of 150% D_W D_n revealed practically identical FIP and FBP, reduced by 24% and 12%, respectively, compared to the baseline open hole.

- For shallow V notches (50% D_W), the theoretical model predicted a FIP value very close to the FIP of a deep U notch (150% D_W). In other words, sharp notches may increase efficiency, while cutting deeper notches is problematic.

Acknowledgments

This article was prepared for presentation at the International Geomechanics Symposium, Abu Dhabi, UAE, November 7-10, 2022.

References

1. Oparin, M., Sadykov, A., Khan, S. and Tineo, R.: "Impact of Local Stress Heterogeneity on Fracture Initiation in Unconventional Reservoirs: A Case Study from Saudi Arabia," SPE paper 181617, presented at the SPE Annual Technical Conference and Exhibition, Dubai, UAE, September 26-28, 2016.

2. Asif, A.B., Hansen, J., Khan, A. and Sheshtawy, M: "Integration of Post-Fracturing Spectral Noise Log, Temperature Modeling, and Production Log Diagnoses Water Production and Resolves Uncertainties in Open Hole Multistage Fracturing," SPE paper 204668, paper prepared for presentation at the SPE Middle East Oil and Gas Show and Conference, event canceled, November 28-December 1, 2021.

3. Bartko, K., Tineo, R., Aidagulov, G., Al-Jalal, Z., et al.: "First Application for a Sequenced Fracturing Technique to Divert Fractures in a Vertical Open Hole Completion: Case Study from Saudi Arabia," SPE paper 179127, presented at the SPE Hydraulic Fracturing Technology Conference, The Woodlands, Texas, February 9-11, 2016.

4. Chang, F.F., Bartko, K., Dyer, S., Aidagulov, G., et al.: "Multiple Fracture Initiation in Open Hole without Mechanical Isolation: First Step to Fulfill an Ambition," SPE paper 168638, presented at the SPE Hydraulic Fracturing Technology Conference, The Woodlands, Texas, February 4-6, 2014.

5. Aidagulov, G., Edelman, E., Brady, D., Gwaba, D., et al.: "Notching as a Novel Promising Technique to Reduce Fracture Initiation Pressure in Horizontal Open Hole Wellbores," paper ARMA-IGS-21-044, presented at the ARMA/DGS/SEG 2nd International Geomechanics Symposium, virtual, November 1-4, 2021.

6. Aidagulov, G., Alekseenko, O., Chang, F.F., Bartko, K., et al.: "Model of Hydraulic Fracture Initiation from the Notched Open Hole," SPE paper 178027, presented at the SPE Saudi Arabia Section Annual Technical Symposium and Exhibition, al-Khobar, Kingdom of Saudi Arabia, April 21-23, 2015.

7. Hubbert, M.K. and Willis, D.G.: "Mechanics of Hydraulic Fracturing," *Transactions of the American Institute of Mining Engineers*, Vol. 210, 1957, pp. 153-168.

8. Detournay, E. and Carbonell, R.: "Fracture Mechanics Analysis of the Breakdown Process in Minifracture or Leakoff Test," *SPE Production & Facilities*, Vol. 12, Issue 3, August 1997, pp. 195-199.

9. Aidagulov, G., Gwaba, D., Kayumov, R., Sultan, A., et al.: "Effects of Preexisting Fractures on Carbonate Matrix Stimulation Studied by Large-Scale Radial Acidizing Experiments," SPE paper 195153, presented at the SPE Middle East Oil and Gas Show and Conference, Manama, Kingdom of Bahrain, March 18-21, 2019.

10. Qiu, X., Aidagulov, G., Ghommem, M., Edelman, E., et al.: "Toward a Better Understanding of Wormhole Propagation in Carbonate Rocks: Linear vs. Radial Acid Injection," *Journal of Petroleum Science and Engineering*, Vol. 171, December 2018, pp. 570-583.

About the Authors

Dr. Murtadha J. AlTammar

Ph.D. in Petroleum Engineering, University of Texas

Dr. Murtadha J. AlTammar is a Petroleum Engineer working with the Production Technology Team of Saudi Aramco's Exploration and Petroleum Engineering Center – Advanced Research Center (EXPEC ARC).

Previously, Murtadha worked in the field for 18 months as a Completion and Production Engineer with the Southern Area Gas Production Engineering Division.

He received the 2011 SAPED Significant Achievement Award for leading a well intervention campaign, and also the 2017 EXPEC ARC Best-in-Class Young Researcher Award. Murtadha was an invited speaker at the 2017 American Rock Mechanics Association (ARMA) Hydraulic Fracturing Workshop in San Francisco, CA.

He has been a technical reviewer for many journals. Murtadha has also been a member of organizing several technical committees for the Society of Petroleum Engineers (SPE) and ARMA conferences.

He received his B.S. degree in Petroleum Engineering from the Colorado School of Mines, Golden, CO. Murtadha received his M.S. degree and Ph.D. degree in Petroleum Engineering, specializing in hydraulic fracturing mechanics, from the University of Texas at Austin, Austin, TX.

Dr. Khalid M. Al-Ruwaili

Ph.D. in Petroleum Engineering (Geomechanics), Heriot-Watt University

Dr. Khalid M. Al-Ruwaili is a Petroleum Engineer leading and supporting several research projects in the Production Technology Division of Saudi Aramco's Exploration and Petroleum Engineering Center – Advanced Research Center (EXPEC ARC).

He joined Saudi Aramco in 2006 as a Petroleum Engineer working in various technical positions for the Northern Area Reservoir Management at Berri field. After this assignment, Khalid worked on the ultimate development plan of the Upper Fadhili reservoir, a tight carbonate reservoir. His area of research is borehole mechanics, wellbore stimulation, hydraulic fracturing, and reservoir geomechanics.

He is an active member of the Society of Petroleum Engineers (SPE) and a technical contributor to the American Rock Mechanics Association. Khalid has authored and coauthored several technical papers.

He received his B.S. degree in Petroleum and Natural Gas Engineering from King Saud University, Riyadh, Saudi Arabia, an M.S. degree in Petroleum Engineering (Geomechanics) from the University of Calgary, Calgary, Alberta, Canada, and a Ph.D. degree in Petroleum Engineering (Geomechanics) from Heriot-Watt University, Edinburgh, Scotland, U.K.

Dr. Gallyam Aidagulov

Ph.D. in Computational Mathematics, Lomonosov Moscow State University

Dr. Gallyam Aidagulov started his Schlumberger career in 2004 as a Scientist when he joined the corporate research center in Moscow, Russia. Since that time, Gallyam has focused on geomechanics through his involvement in various projects where he applied and further developed his expertise in computational mechanics for development of theoretical and numerical models of such processes as proppant flow back, sanding, fault reactivation and reservoir rock failure localization.

In March 2012, he moved to the Schlumberger Carbonate Research Center in Dhahran, Saudi Arabia, to work on fracture and acid stimulation challenges

Gallyam has authored or coauthored 30+ publications in leading industrial conferences and journals on the subjects of applied mathematics, numerical modeling, geomechanics, reservoir stimulation, and lab and field experimentation. He has also co-invented more than 10 international granted and filed patent applications.

In 2000 and 2004, Gallyam received his M.S. and Ph.D. degrees, respectively, in Computational Mathematics from the Lomonosov Moscow State University, Moscow, Russia.

Hussain K. Al-Dakheel

M.S. in Mechanical Engineering, King Fahd University of Petroleum and Minerals

Hussain K. Al-Dakheel is a Research Engineer at the Schlumberger Dhahran Carbonate Research Center (SDCR) working with the Production and Completion group. Before joining the SDCR, he worked in Schlumberger's coiled tubing (CT) services segment for 4 years as a Field Engineer where he designed, prepared, and executed CT jobs that include acid stimulation and unconventional gas well interventions.

Hussain is the author/coauthor of several published works and patent applications on multidisciplinary subjects, such as material science and petroleum engineering.

He received his B.S. degree in Mechanical Engineering from King Fahd University of Petroleum and Minerals (KFUPM), Dhahran, Saudi Arabia, and his M.S. degree (first honor) in Mechanical Engineering, also from KFUPM.

Dr. Devon C. Gwaba

Ph.D. in Civil and Geotechnical Engineering, Georgia Institute of Technology

Dr. Devon C. Gwaba is currently the Geotechnical Department Manager for the Intertek-PSI office in Nashville, TN, U.S. In this role, Devon provides advanced technical work execution and supports business development, leading a multidisciplinary team of engineers and scientists working on several horizontal directional drilling for pipeline projects in the U.S.

Before joining Intertek-PSI, he was a Senior Civil Forensic Engineer for Exponent Engineering and Scientific Consulting where he conducted several international investigations on engineering failures.

From 2016 to 2021, Devon was a Geomechanics Research Scientist at Schlumberger's Dhahran Carbonate Research Center in Saudi Arabia. As part of the Production and Completions team, he delivered innovative experimental research, exploring ways of enhancing reservoir production, drilling, and completions operations. Devon's expertise in geomechanics testing tools enabled him to act as a bridge between laboratory-scale testing and field application of geomechanics to deliver novel insights into local challenges.

Devon has authored or coauthored several publications in reputable journals. He also holds or jointly holds more than five patents.

Devon is also a licensed professional engineer (PEng) in the State of Georgia where he has authored or coauthored several geotechnical reports for both the private and the public sector.

In 2006, Devon received his M.S. degree, and in 2016, he received his Ph.D. degree, both in Civil and Geotechnical Engineering from the Georgia Institute of Technology, Atlanta, GA.

Dr. Mustapha Abbad

Ph.D. in Mechanical Engineering, Ecole Nationale Supérieure d'Electricité et de Mécanique

Dr. Mustapha Abbad is currently the Research Program Manager leading the Production and Completions group in Schlumberger's Dhahran Carbonate Research Center, managing the research themes on acid and fracturing stimulation, and downhole sensing for smart completions research. He has been in this position since 2017.

Previously, from 2003 to 2007, Mustapha worked as a Scientist and Teaching Professor in academic institutions in France where he conducted theoretical and experimental modeling of complex multiphase flows for medical and industrial research collaborators.

After joining Schlumberger in 2007 as a Scientist at the Dhahran Carbonate Research Center, Mustapha continued his hydrodynamics research — now for petroleum applications via numerical simulations, as well as building and experimenting in multiphase flow loops, separators, diversion solutions for stimulation, and smart completions.

Mustapha is the author and coauthor of numerous technical contributions, published in leading industrial conferences and journals, as well as in internationally filed and granted patent applications.

In 1998, he received his M.S. degree, and in 2003, he received his Ph.D. degree, both in Mechanical Engineering from Ecole Nationale Supérieure d'Electricité et de Mécanique, INP de Lorraine, Nancy, France.